

Epitaxial Growth and Ferroelectric Properties of PbTiO₃ Thin Films on Coherently Grown Pt Bottom Electrodes

Hironori Fujisawa, Masayoshi Kume and Masaru Shimizu

Department of Electrical Engineering and Computer Sciences, Graduate School of Engineering, University of Hyogo, 2167 Shosha, Himeji, Hyogo 671-2201, Japan

Fax: 81-79-267-4855, e-mail: fujisawa@eng.u-hyogo.ac.jp

We investigated epitaxial growth of PbTiO₃ thin films on coherent and incoherent Pt thin films on SrTiO₃(100) by metalorganic chemical vapor deposition and their ferroelectric properties. PbTiO₃ films were grown on both Pt films in the Volmer-Weber mode. The coalescence of neighboring islands observed at the earlier growth stage on coherent Pt films than on incoherent Pt films due to the higher crystalline orientation and smoother surface. Therefore, the minimum thickness above which continuous PbTiO₃ films were formed on coherent Pt films, 50nm, was smaller than 100nm on incoherent Pt films. 50nm-thick PbTiO₃ films on coherent Pt films showed D-E hysteresis loops with a remanent polarization of 64.0μC/cm² and a coercive field of 275kV/cm.

Key words: epitaxial growth, PbTiO₃, coherent Pt films

1. INTRODUCTION

For epitaxial growth of ferroelectric thin films, many kinds of substrate and electrode materials have been used. Among various materials, SrRuO₃ (SRO) is one of the most promising materials because coherently grown films with an atomically controlled surface can be obtained on SrTiO₃ (STO) single crystal. [1] There have been many reports on epitaxial growth of ferroelectric thin films on SRO/STO. By using SRO/STO, single-crystalline PbTiO₃ thin films have been successfully prepared by off-axis sputtering [2] and hydrothermal method. [3] In these reports, ferroelectric properties of PbTiO₃ films have been also examined at film thicknesses down to 100nm [2,3] although it had been quite difficult to obtain pure PbTiO₃ crystals with a high crystallinity and high resistivity due to a high volatility of lead oxide (PbO_x) and a phase transition from cubic to tetragonal phase during cooling after the crystallization. This means that bottom electrodes with high crystallinity are inevitable for electrical measurements of PbTiO₃ thin films.

In addition to SRO on STO, epitaxial Pt films grown on STO and MgO have also been used as bottom electrodes for epitaxial ferroelectric thin films. [4-7] However, it has been quite difficult to obtain single-crystalline Pt thin films with an atomically flat surface because a large amount of misfit dislocations was introduced into the film/substrate interface. This is one of reasons why SRO has been favored as a bottom electrode for epitaxial growth of ferroelectric thin films although polycrystalline Pt films were very often used. Therefore, the crystallinity of PbTiO₃ thin films on Pt bottom electrodes has not been so high as that of those on SRO bottom electrodes. For example, the thickness of epitaxial PbTiO₃ thin films on Pt bottom electrodes in which D-E hysteresis loops have been successfully observed, 1μm, was much larger than those of films on SRO. [6,7]

Recently, we have successfully obtained coherently grown Pt(001) thin films on STO(100) single crystals up to thicknesses of 60nm by inserting very thin (<1nm) Ir layers into Pt/STO interface. [8] The coherent Pt films showed an atomically flat surface, and a smaller misfit dislocation density than relaxed Pt films with thicknesses larger than 100nm. Therefore, the coherent Pt films can be a new candidate as bottom electrodes for preparation of epitaxial ferroelectric films.

In this study, we investigate epitaxial growth of PbTiO₃ thin films on coherently strained Pt bottom electrodes by metalorganic chemical vapor deposition (MOCVD). Ferroelectric properties of PbTiO₃ thin films are also discussed.

2. EXPERIMENTAL PROCEDURE

STO(100) single crystals were used as a substrate. In order to obtain an atomically flat surface with TiO₂-termination, STO was etched in a buffered NH₄F-HF solution and subsequently annealed at 950°C in air. [9] Pt and Ir thin films were prepared at 550°C in an Ar pressure of 10mTorr by rf magnetron sputtering. Deposition rates of Pt and Ir films were 40 and 6.0nm/min, respectively. The coherently grown Pt films with a thickness of 30nm were prepared on STO(100) by inserting 0.5nm-thick Ir layer into the interface between Pt and STO(100). The 100nm-thick relaxed Pt films were directly prepared on STO(100). PbTiO₃ films were prepared on these two types of Pt electrodes by MOCVD. The growth temperature and pressure were 540°C and 5.0Torr, respectively. (C₂H₅)₃PbO-*n*-CH₂C(CH₃)₃, Ti(O-*i*-C₃H₇)₄ and O₂ were used as precursors and oxidant, respectively. The thickness of PbTiO₃ films was controlled by changing the deposition time. The growth rate calculated from a thickness of PbTiO₃ film deposited for 20min was 6.8nm/min. Crystalline properties and film thicknesses were evaluated by x-ray diffraction (XRD) and scanning

electron microscopy. In-plane and out-of-plane lattice parameters were determined by XRD-reciprocal space mapping around STO (003) and (103) diffraction spots. The surface morphology and domain structure were observed by an atomic force microscopy (AFM) and piezoresponse force microscopy (PFM). For electrical measurements, 100nm-thick Pt top electrodes with a diameter of $50\mu\text{m}$ were prepared by sputtering and lift-off process. D-E hysteresis loops and switching currents were measured by the Sawyer-Tower circuit and a digitizing oscilloscope.

3. RESULTS AND DISCUSSION

3.1 Growth of coherent and incoherent Pt films

STO is a cubic perovskite with a lattice parameter of 0.3905nm. Pt and Ir are face-centered-cubic metals with lattice parameters of 0.3923 and 0.3841nm, respectively. Therefore, Pt films on STO(100) will be under compressive stress in the in-plane from a mismatch with substrate at both room and growth temperatures. The critical thickness below which Pt films coherently grown on STO(100) substrate at the growth temperature of 550°C is calculated to be 22nm using the mechanical equilibrium theory by Matthews et al. [10] Therefore, when Pt films with thicknesses larger than 50nm were directly prepared on STO(100), in-plane and out-of-plane lattice parameters of Pt were almost constant at 0.3912 and 0.3943nm, respectively, independently of the thickness. The in-plane lattice parameter was larger than that of STO and smaller than that of bulk Pt. This means that Pt films with thicknesses above 50nm were partially relaxed. On the other hand, when a very thin Ir layer ($\sim 0.5\text{nm}$) was inserted into the interface between Pt and STO substrate, the in-plane lattice constant of Pt films was equal to 0.3905nm of STO up to the thickness of 60nm. This indicates that Pt films were coherently grown on STO and the critical thickness increased to 60nm. According to the Vegard's rule, the lattice parameter of Pt-Ir alloy will be more close to that of STO than those of Pt or Ir because Pt and Ir have slightly larger (+0.5%) and smaller (-1.7%) lattice parameters than that of STO, respectively. Therefore, it is concluded that the formation of the alloy of Pt and Ir reduced the generation of misfit dislocations at the interface.

Topographic AFM images of partially relaxed 100nm-thick Pt and coherent 20nm-thick Pt/Ir films are shown in Fig.1. The 100nm-thick Pt film showed a

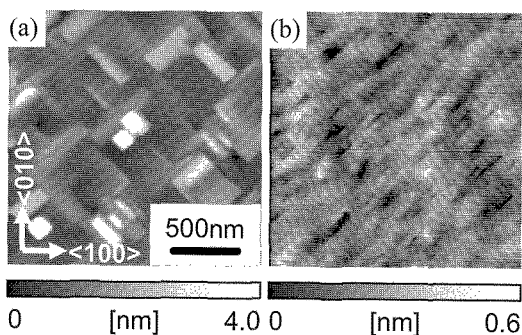


Fig.1 AFM images of (a) incoherent 100nm-thick Pt and (b) coherent 20nm-thick Pt/Ir films.

rough surface with a root-mean-square (rms) surface roughness of 0.6nm. The cross-hatch pattern observed along the $\langle 110 \rangle$ direction corresponds to the generation of misfit dislocations. The surface morphology of the coherent Pt/Ir films was largely different from that of incoherent Pt films. Atomic steps with a height of 0.2nm, corresponding to one half of Pt unit cell, were clearly observed on the surface. An rms surface roughness was less than 0.1nm.

XRD measurements revealed that full widths at a half maximum (FWHMs) of rocking curves of Pt(002) diffraction peaks were 0.3° for incoherent Pt and 0.06° for coherent Pt/Ir films. This indicates that the crystallinity of coherent Pt/Ir films was much higher than that of incoherent Pt films.

On the other hand, the crystallinity of Pt films was degraded when the thickness of Ir layers was larger than 1nm. Details of preparation of coherent Pt/Ir films will be published elsewhere.

3.2 Epitaxial growth of PbTiO_3 films

PbTiO_3 thin films with thicknesses from 34 to 136nm were prepared on these two types of Pt films by MOCVD. The thicknesses were changed by changing the deposition time from 5 to 20min. Epitaxial growth of PbTiO_3 films was confirmed by pole figure measurements of $\text{PbTiO}_3(101)$, Pt(202) and STO(202) diffractions. AFM observations revealed 3-dimensional island formation with a subsequent coalescence of neighboring islands at the early growth stage of PbTiO_3 films on both Pt films. This means that the growth mode of PbTiO_3 on Pt is the Volmer-Weber (V-W) mode independently of the in-plane lattice constants, crystallinity or surface roughness of Pt films. [11] Film growth of PbTiO_3 on Pt/Ir and Pt films was different in

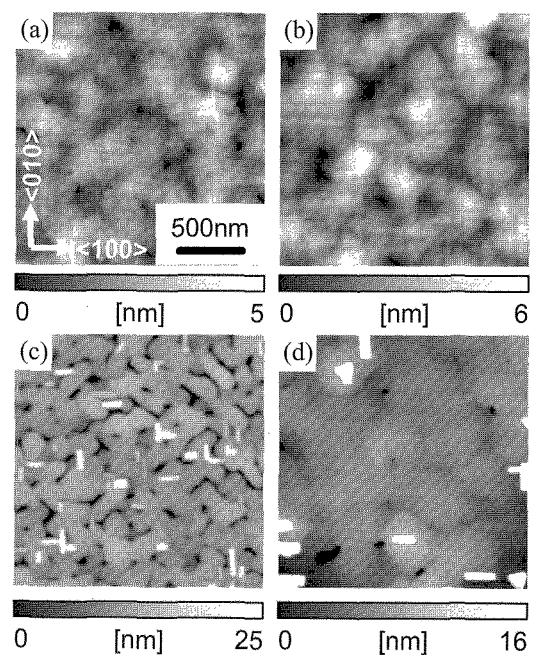


Fig.2 AFM images of PbTiO_3 films grown on (a, b) coherent Pt/Ir and (c,d) incoherent Pt films. Deposition times and thicknesses are (a,c) 7.5 min and 50nm, and (b,d) 15min and 100nm, respectively.

the formation of continuous films from small islands; the coalescence occurred at earlier growth stage on Pt/Ir films than on Pt films. Therefore, continuous films were formed on Pt/Ir films when deposition times were longer than 7.5min, as shown in Fig.2. The minimum thickness above which continuous films were formed was 50nm. On the other hand, continuous films were obtained on relaxed Pt films when deposition times were longer than 15min, corresponding to a thickness of 100nm. This difference indicates that the coalescence of neighboring islands more easily occurred on coherent Pt/Ir films than on incoherent Pt films because of their smoother surface. In addition, pyramidal-shaped and triangular-prism-shaped nanoislands were observed on the continuous PbTiO₃ films on the incoherent Pt films, as shown in Figs.2(c,d). Due to this difference in the film growth, the surface roughness of PbTiO₃ on Pt/Ir films, 0.9-1.9nm, was much smaller than 4.4-6.5nm of PbTiO₃ on Pt films. These AFM observations revealed that the growth behavior of PbTiO₃ thin films was largely influenced by the surface roughness of underlying bottom electrodes or substrates even in the V-W growth mode. AFM and PFM observations also revealed *a-c* multidomain structure in continuous PbTiO₃ films on Pt and Pt/Ir films. The generation of *a-c* multidomains is also confirmed by XRD measurements of PTO(001) and (100) diffractions.

The in-plane and out-of plane lattice parameters of *c*-domains in 100nm-thick PbTiO₃ films on Pt/Ir films were 0.392 and 0.411nm, respectively. The lattice parameters of continuous PbTiO₃ films showed no distinct dependence on the film thickness. PbTiO₃ thin films on incoherent Pt films showed the nearly same lattice parameters as those of PbTiO₃ on coherent Pt/Ir films. This means that the extent of relaxation of strains from a mismatch of thermal expansion coefficients of PbTiO₃ and STO was not dependent on the coherency of underlying Pt films, and that the strain due to the lattice mismatch between cubic PbTiO₃ and Pt at the growth temperature was relaxed by the generation of misfit dislocations at the interface. [12] In addition, no distinct difference was observed for FWHMs of rocking curves of the PbTiO₃(001) peak of continuous films on both coherent Pt/Ir and incoherent Pt films. From these XRD measurements, it is found that there was no distinct difference in the crystallinity of continuous PbTiO₃ films on both coherent Pt/Ir and incoherent Pt films because the thickness was much larger than the critical thickness for coherent growth of PbTiO₃ on both Pt films.

3.3 Ferroelectric properties of PbTiO₃ thin films

D-E hysteresis loops can be obtained for continuous PbTiO₃ films on both Pt/Ir and Pt bottom electrodes, as shown in Fig.3. Remanent polarization (*P_r*) and coercive field (*E_c*) were 60.3μC/cm² and 184kV/cm, and 61.0μC/cm² and 195kV/cm for 100nm-thick PbTiO₃ films on incoherent and coherent Pt, respectively. The *P_r* and *E_c* of the 50nm-thick PbTiO₃ film were 64.0μC/cm² and 275kV/cm, respectively. The *P_r* values were determined by switching current measurements in which leakage currents can be subtracted because the leakage was observed in D-E loops shown in Fig.3; the *E_c* values were obtained from D-E loops. The difference in

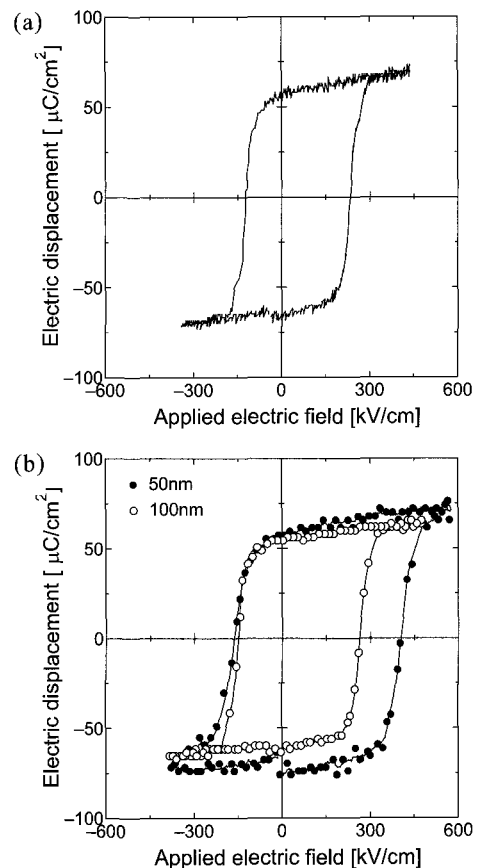


Fig.3 D-E hysteresis loops of (a) 100nm-thick PbTiO₃ film on incoherent Pt and (b) 50 and 100nm-thick PbTiO₃ films on coherent Pt bottom electrodes, respectively.

P_r values corresponds to the difference in the volume fraction of *c*-domain. The fractions determined by the XRD measurements were 94 and 85% for 50 and 100nm-thick PbTiO₃ films on Pt/Ir and 84% for 100nm-thick PbTiO₃ on Pt, respectively, indicating that fraction was dependent on the thickness not on the coherency of the Pt bottom electrodes. These *P_r* values are comparable with previously reported values for PbTiO₃ films prepared above the Curie temperature (*P_r*=80μC/cm² for 1μm-thick film prepared on Pt/MgO(100) at 550°C by pulsed laser ablation, [6,7], *P_r*=40μC/cm² for 125nm-thick film on SRO/STO(100) at 600-700°C by off-axis sputtering [2], and *P_r*=96.5μC/cm² for perfectly *c*-axis oriented 100nm-thick films on SRO/STO(100) by the hydrothermal method at 150°C [3]). The thickness of 50nm in which saturated D-E hysteresis loops were successfully obtained is the minimum value among PbTiO₃ films prepared on SRO and Pt bottom electrodes previously reported. [2-7] These results indicate that the Pt films coherently grown on STO(100) can be used as a bottom electrode for epitaxial growth of ferroelectric thin films.

4. CONCLUSIONS

Coherently grown Pt films with thicknesses up to 60nm were successfully prepared on STO(100) by

inserting very thin Ir layer into the Pt/STO interface. Coherent Pt films showed a step and terrace structure with a 0.2nm-high atomic step, corresponding to a half unit cell of Pt. The minimum thicknesses above which PbTiO₃ formed continuous films were 50 and 100nm on coherent Pt/Ir and incoherent Pt films, respectively. 50nm-thick PbTiO₃ films on coherent Pt/Ir films showed saturated hysteresis loops with a Pr of 64.0μC/cm². From these experimental results, it is demonstrated that coherent Pt/Ir films on STO(100) is a new candidate as bottom electrodes for epitaxial growth of ferroelectric thin films.

ACKNOWLEDGEMENTS

This work was supported in part by a Grant-in-Aid for Young Scientists (B) (18760238) from the Ministry of Education, Culture, Sports, Science and Technology, a Grant-in-Aid from the Japan Society for the Promotion of Science (B) (17360144), and research grants from the Sumitomo Foundation.

References

- [1] C. B. Eom, R. J. Cava, R. M. Fleming, J. M. Phillips, R. B. Dover, J. H. Marshall, J.W. P. Hsu, J. J. Krajewski and W. F. Peck Jr., *Science*, **258**, 1766-1769 (1992).
- [2] K. Wasa, Y. Haneda, T. Sato, H. Adachi and I. Kanno, *Integrated Ferroelectrics*, **21**, 451-460 (1998).
- [3] T. Morita and Y. Cho, *Appl. Phys. Lett.*, **85**, 2331-2333 (2004).
- [4] W. J. Takei, N. P. Formigoni, and M. H. Francombe, *Appl. Phys. Lett.*, **15**, 256-258 (1969).
- [5] Y. Sakashita, H. Segawa, K. Tominaga and M. Okada, *J. Appl. Phys.*, **73**, 7857-7863 (1993).
- [6] H. Tabata, O. Murata, T. Kawai, S. Kawai and M. Okuyama, *Jpn. J. Appl. Phys.*, **32**, 5611-5614 (1993).
- [7] H. Tabata, O. Murata, T. Kawai, S. Kawai and M. Okuyama, *Appl. Phys. Lett.*, **64**, 428-430 (1994).
- [8] H. Fujisawa, M. Kume, M. Shimizu, Y. Kotaka and K. Honda, *Draft of Proceedings of the 16th IEEE International Symposium on the Applications of Ferroelectrics*, 29-PS-A-3 (Nara, Japan, May 27-31, 2007).
- [9] G. Koster, B. L. Kropman, G. J. H. M. Rijnders, D. H. A. Blank and H. Rogalla, *Appl. Phys. Lett.*, **73**, 2920-2922 (1998).
- [10] J. W. Matthews and A. E. Blakeslee, *J. Cryst. Growth*, **27**, 118-125 (1974).
- [11] M. Shimizu, H. Fujisawa, H. Niu and K. Honda, *J. Cryst. Growth*, **237-239**, 448-454 (2002).
- [12] J. S. Speck and W. Pompe, *J. Appl. Phys.*, **76**, 466-476 (1994).

(Received December 10, 2007; Accepted January 29, 2008)